The 11th IEEE International Workshop on
Advanced Motion Control
March 21-24, 2010, Nagaoka, Japan

Compensation for Synchronous Component of Angular Transmission Errors in Harmonic Drive Gearings

Masafumi Yamamoto,
Makoto Iwasaki,
Makoto Kainuma
Nagoya Institute of Technology
Dept. of Comp. Sci. & Eng.
Gokiso, Showa, Nagoya, 4668555, JAPAN
Email: yama@position.elcom.nitech.ac.jp

Yoshifumi Okitsu,
Kato Yuki,
Kozo Sasaki,
Toshio Yajima
Harmonic Drive Systems Inc.
Minami-Oi, Shinagawa-ku, Tokyo, 1400013, JAPAN

***Abstract*— This paper presents a modeling and compensation methodology for angular transmission errors in harmonic drive gearings. In this research, effects of synchronous component in the transmission error on the positioning performance are analytically examined. On the basis of the examinations, a transmission error model-based feedforward compensation is adopted to improve the positioning performance during both static and dynamic positioning motions. The proposed approach has been verified by experiments using a prototype with harmonic drive gearings.**

I. Introduction

Harmonic drive gearings are widely used in a variety of industrial applications, e.g. industrial robots, precision positioning devices, etc., because of its unique kinematics, simple, compact mechanism, high gear ratios, high torque and zero backlash[1]. Fig.1 shows components of the harmonic drive gearing. This transmission system is generally comprised of just three components: a wave generator (WG) with an elliptical shape, a flexspline (FS) of an elastic thin-walled stell cup, and a circular spline (CS) of a rigid steel ring with internal teeth, which was developed to take advantages of the elastic dynamics of metal. Typical mechatronic devices including harmonic drive gearings, such as industrial robots, are generally controlled in a semi-closed control manner. However, since the transmission systems inherently possess nonlinear attributes known as 'angular transmission errors' due to the structural error and flexibility, the ideal control accuracy corresponding to the apparent resolution cannot be attained in the load side[2], [3], [4], [5], [6].

Under the background above, this paper presents a novel compensation for the synchronous component of angular transmission errors to improve the static and dynamic positioning performance in a semi-closed control manner. The authors have already discussed to improve the static positioning performance by a model-based feedforward compensation, where the dynamic positioning performance has not been considered[7], [8]. In many conventional researches considering the dynamic positioning performance, although the vibration suppression has been mainly discussed, which was caused by the nonlinear stiffness due to flexibility of the flexspline, most of them have not considered effects of the synchronous components[9], [10], [11], [12]. In this research, therefore, the effects of the synchronous component in transmission errors on both static and dynamic positioning performance are analytically examined and compensated. The proposed approach has been verified by experiments using a prototype with harmonic drive gearings.

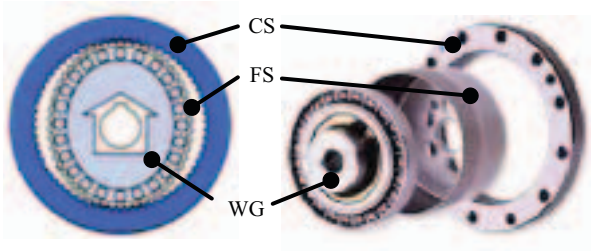

Fig. 1. Components of harmonic drive gearing.

II. Configuration of Experimental Setup

Fig.2 shows a schematic configuration of laboratory prototype as an experimental positioning device, which is comprised of an actuator (AC motor) with an encoder, a harmonic drive gearing, an inertial load, and a load side encoder. Specifications of the prototype are listed in Table I. This positioning device is controlled in a typical semi-closed control manner by an angular feedback with the encoder mounted on motor shaft, while the load side encoder measures and evaluates the load angle. Inertia ratio between the actuator and the load is about 1 : 3 on the motor shaft.

III. Modeling of Actuator with Synchronous Component

A. Modeling for synchronous component

The angular transmission error θ_{TE} is generally defined by a motor angle θ_m, a load angle θ_l, and a gear ratio N as follows[4].

$$\theta_{\mathrm{TE}} = \theta_l - \theta_m/N \tag{1}$$

The synchronous component θ_{Sync} is basically caused by kinematic errors in teeth of FS and CS, and assembling errors in shaft of gearing and load, which is synchronous

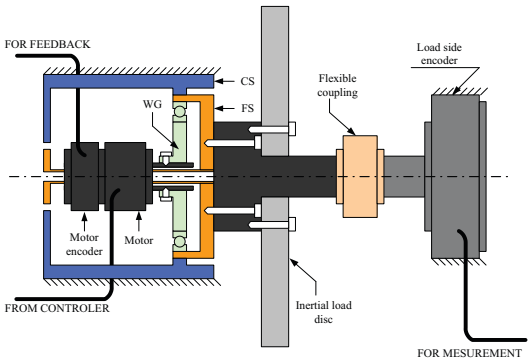

Fig. 2. Experimental setup.

TABLE I
SPECIFICATIONS OF PROTOTYPE.

gear ratio (N)	50
FS tooth number (z_f)	100
CS tooth number (z_c)	102
motor encoder resolution	8,000 pulse/rev
load encoder resolution	2,880,000 pulse/rev

to the relative rotation of WG, FS, and CS. In this research, only θ_{TEM}, which is synchronous competent to motor angle, is modeled as $\theta_{\mathrm{Sync}}(\theta_m)$, since the load angle cannot be detected for the positioning control. The synchronous component, therefore, is mathematically formulated as the following periodical pulsation for θ_m:

$$\theta_{\mathrm{Sync}}(\theta_m) = \sum_{i=1}^{n_m} A_m(i) \cos(i\theta_m + \phi_m(i)), \qquad (2)$$

where i: harmonic order for motor angle, A_m: amplitude of harmonics, and ϕ_m: phase of harmonics.

Fig.3 shows experimental waveforms and spectrum analyses of the synchronous component. The transmission error waveforms in the upper figure are indicated by the measured θ_m and θ_l for one revolution of load with a fine inching motion (step amplitude of 3.6°) in clockwise (CW) direction, where the horizontal axis of load angle is magnified to scale three revolutions of motor (1deg = 3600 arc-sec in load angle). The solid lines in the lower figure are spectrum amplitudes of the experimental waveforms for the harmonic order. In the parameterization of $A_m(i)$ and $\phi_m(i)$, the dominant components in the spectrum amplitudes have been extracted, where larger components than a threshold indicated by a horizontal dashed line in the figure have been parameterized in (2). The blue thick lines in the lower figure indicate the modeled spectrum amplitudes of harmonics. The blue dashed line in the upper figure indicates the waveform of the synchronous component model. From the figure, the model can precisely reproduce the actual synchronous component of transmission errors.

B. Modeling for actuator

Positioning mechanism with the harmonic drive gearing can be generally modeled as a two-inertia system. Fig.4 shows a block diagram of the mechanism as a plant, where J_m: inertia of motor, D_m: damping of motor, J_l: inertia of load, D_l: damping of load, K_g: stiffness of gearing, D_g: damping of gearing, K_t: torque constant, ω_m: velocity of motor, ω_l: velocity of load, and i_{ref}: current reference. In this mathematical model, the synchronous component θ_{Sync} of transmission errors is modeled as an angular disturbance for the torsional angle of $(\theta_m/N - \theta_l)$.

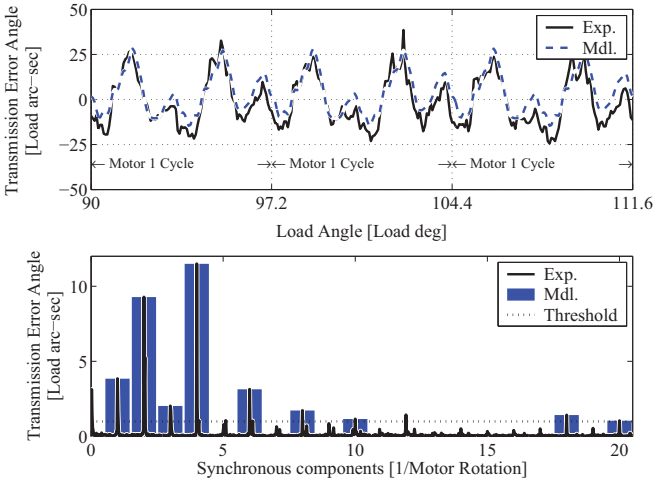

Fig. 3. Modeling results of synchronous components (CW).

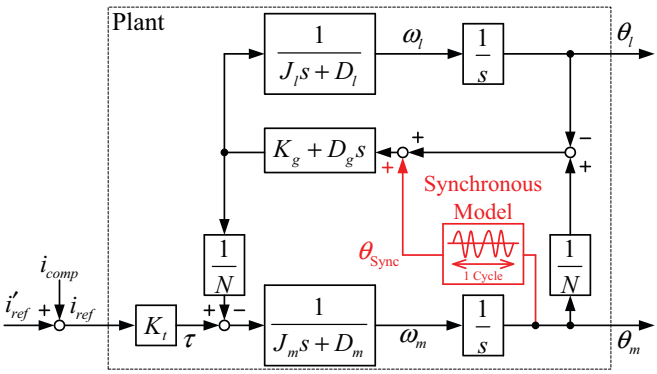

Fig. 4. Block diagram of positioning mechanism with synchronous component of transmission errors.

IV. COMPENSATION FOR SYNCHRONOUS COMPONENT

In this compensation approach, the synchronous component model has been adopted to the positioning system as a model-based feedforward compensation manner, in order to improve the static and dynamic positioning performance. Fig.5 shows a block diagram of 2-degrees-of-freedom controller with the synchronous component compensation, where Plant: plant model as of Fig.4, $C(s)$: feedback compensator, $D(s)$, $N(s)$: feedforward compensators, i^*_{ref}: feedforward current reference, θ^*_m: feedforward position reference, θ_{Err}: error of motor position, i_{comp}: additional motor current reference for compensation, θ_{comp}: compensation angular signal for motor, and r: original position reference. The desired positioning performance in the load side can be achieved by i_{comp}, while the motor angle is also affected by i_{comp}. The motor angle reference, therefore, is corrected by θ_{comp} to allow θ_{Err} = 0 under the ideal condition without modeling errors and disturbances.

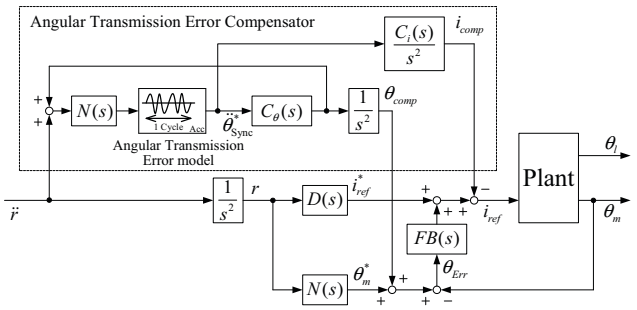

Fig. 5. Block diagram of 2-degrees-of-freedom controller with synchronous component compensator.

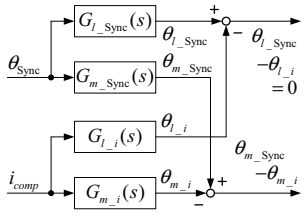

Fig. 6. Block diagram of compensation current command i_{comp} for synchronous components $\theta_{\rm Sync}$.

Fig.6 shows a block diagram of i_{comp} for $\theta_{\rm Sync}$. In the figure, $G_{m\_\rm Sync}(s)$ and $G_{l\_\rm Sync}(s)$ are transfer functions of θ_m and θ_l for $\theta_{\rm Sync}$, and $G_{m\_i}(s)$ and $G_{l\_i}(s)$ are transfer functions of θ_m and θ_l of i_{comp}:

$$G_{m\_\rm Sync}(s) = \frac{\theta_{m\_\rm Sync}(s)}{\theta_{\rm Sync}(s)} \quad (3)$$

$$G_{l\_\rm Sync}(s) = \frac{\theta_{l\_\rm Sync}(s)}{\theta_{\rm Sync}(s)} \quad (4)$$

$$G_{m\_i}(s) = \frac{\theta_{m\_i}(s)}{i_{comp}(s)} \quad (5)$$

$$G_{l\_i}(s) = \frac{\theta_{l\_i}(s)}{i_{comp}(s)} \quad (6)$$

Here, $\theta_{l\_\rm Sync}$ can be compensated by i_{comp} under $\theta^*_{\rm Sync} = \theta_{\rm Sync}$ as follows.

$$\begin{aligned} G_{l\_\rm Sync}(s)\theta_{\rm Sync}(s) &= G_{l\_i}(s)i_{comp}(s) \\ &= G_{l\_i}(s)C_i(s)\theta^*_{\rm Sync}(s) \quad (7) \\ C_i(s) &= G_{l\_\rm Sync}(s)/G_{l\_i}(s) \quad (8) \end{aligned}$$

Since the relative order of $C_i(s)$ is -2, a filter should be adopted to allow the compensator to be proper. The filter, however, deteriorates the compensation performance due to the delay in higher frequency range. In this case, since the synchronous component can be modeled by a sinusoidal function as described in III-A, the second-order derivative of synchronous function $\ddot{\theta}^*_{\rm Sync}(t)$ is introduced to arrange the second-integration of $C(s)/s^2$ as follows:

$$\begin{aligned} i_{comp}(s) &= C_i(s)\theta^*_{\rm Sync}(s) \\ &= C_i(s)\mathcal{L}\left(\theta^*_{\rm Sync}(t)\right) \\ &= \frac{C_i(s)}{s^2}\mathcal{L}\left(\ddot{\theta}^*_{\rm Sync}(t)\right) \\ &= \frac{C_i(s)}{s^2}\ddot{\theta}^*_{\rm Sync}(s) \quad (9) \end{aligned}$$

$\ddot{\theta}^*_{\rm Sync}(t)$ can be calculated as follows.

$$\begin{aligned} \ddot{\theta}^*_{\rm Sync}(t) &= -\ddot{\theta}_m(t)\sum_{k=1}^{n} kA_k \sin(k\theta_m(t)+\phi_k) \\ &\quad -\dot{\theta}^2_m(t)\sum_{k=1}^{n} k^2A_k \cos(k\theta_m(t)+\phi_k) \quad (10) \end{aligned}$$

θ_{comp}, on the other hand, can be calculated in the same manner as of i_{comp}, under the conditions that $\theta_{Err} = 0$, $\theta_{comp}(s) = \theta_{m\_\rm Sync}(s) + \theta_{m\_i}(s)$, θ_{comp}, as shown in Fig.5

$$\begin{aligned} \theta_{comp}(s) &= \theta_{m\_\rm Sync}(s) + \theta_{m\_i}(s) \\ &= G_{m\_\rm Sync}(s)\theta_{\rm Sync}(s) + G_{m\_i}(s)\frac{C_i(s)}{s^2}\ddot{\theta}^*_{\rm Sync}(s) \\ &= \frac{1}{s^2}\left(G_{m\_\rm Sync}(s) + s^2G_{m\_i}(s)\frac{C_i(s)}{s^2}\right)\ddot{\theta}^*_{\rm Sync}(s) \\ &\equiv \frac{1}{s^2}C_\theta(s)\ddot{\theta}^*_{\rm Sync}(s) \quad (11) \end{aligned}$$

V. Experiment Verifications

In the following experimental verifications, inching motion with amplitude of 12.1 revolutions in motor angle is evaluated to discuss the static positioning performance. The other motion with amplitude of 12.0 revolutions in motor angle is also evaluated to discuss the dynamic positioning performance (240 steps and an interval period of 1.5 s for every step) for CW direction. Notice here that the inching step amplitude of 12.1 was intentionally given in order to provide a different transmission error profile of synchronous component in each inching motion, while the inching step amplitude of 12.0 was given in order to provide the same transmission error of synchronous component in each inching motion.

A. Experimental Results

1) Experiments for Evaluation of Static Positioning Performance: Fig.7 shows waveforms of the static positioning performance in motor angle, load angle, and load acceleration responses, where left side figures indicate the responses without compensation, right side figures indicate the responses with the proposed compensation, and thick blue and red lines represent average responses of each response. By superimposing the compensation θ_{comp} in the motor position reference, the scatted load angle responses can be suppressed.

In order to quantitatively verify the compensation performance, statistical 3σ and mean values for the steady-state error in load angle have been evaluated for each trial. Table II lists a comparison of compensation performance with and without compensation corresponding to Fig.7, where the first row in each value denotes the absolute value and the second row denotes the relative value which is normalized by the value without compensation. As the result of evaluation in 3σ values, the scattered settling accuracy can be successfully reduce about 63% by the proposed compensation.

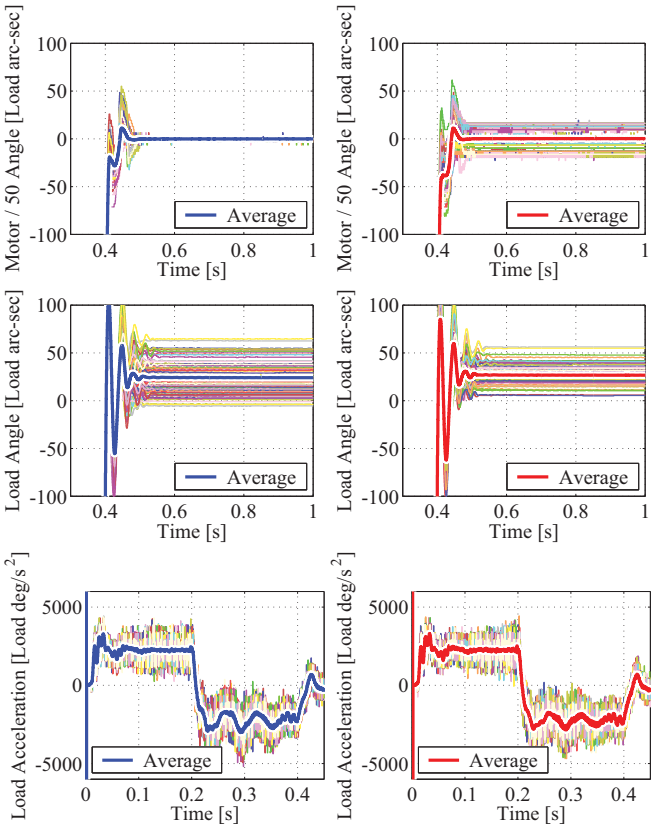

Fig. 7. Response waveforms for target angle of 12.1 motor revolutions.

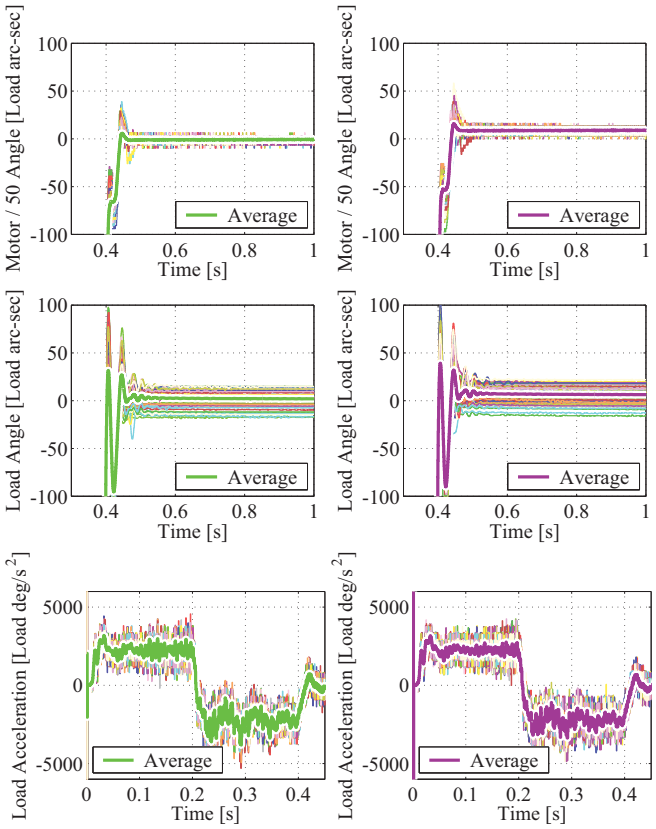

Fig. 8. Response waveforms for target angle of 12.0 motor revolutions.

TABLE II

COMPARISON OF COMPENSATION PERFORMANCE FOR TARGET ANGLE OF 12.1 MOTOR REVOLUTIONS.

	w/o comp.	w/ comp.	
3σ	49.2	31.2	arc−sec
	100	63	%
mean	24.1	26.7	arc−sec
	100	111	%

TABLE III

COMPARISON OF COMPENSATION PERFORMANCE FOR TARGET ANGLE OF 12.0 MOTOR REVOLUTIONS.

	w/o comp.	w/ comp.	
3σ	25.9	25.5	arc−sec
	100	98	%
mean	1.8	6.1	arc−sec
	100	333	%

2) Experiments for Evaluation of Dynamic Positioning Performance: Fig.8, on the other hand, shows waveforms of the dynamic positioning performance in motor angle, load angle, and load acceleration responses, while Table III lists a comparison of compensation performance with and without compensation. Notice here that the scatter in load angle becomes smaller than the one of static positioning performance case, because the synchronous component gives the same effects in every inching motion. On the other hand, the vibration in load acceleration responses in lower figures can be suppressed by the proposed compensation, especially during $0.1 \sim 0.2$ s.

VI. CONCLUSION

This paper proposed the compensation approach for the synchronous component of angular transmission errors to improve both static and dynamic positioning performances in harmonic drive gearings. Experimental results using a laboratory positioning device verified the effectiveness of the proposed compensation. As the result of the proposed compensation, the scattered settling accuracy in load angle can be reduce about 63%, and vibration of load acceleration responses can be suppressed.

REFERENCES

[1] Y. Kiyosawa, and J. Kurogi: Introduction of Ultra Flat Strain Wave Gearing, The JSME international conference on motion and power transmissions, (2004), 76–79 (in Japanese)

[2] Y. Kiyosawa, Xin-yue Zhang, H. Asawa, M. Kato, and K. Inoue: On The Reduction of Tosional Vibration of Strain Wave Gearing(1st Report, High Precision Measurement of Rotational Transmission Error), Transactions of the Japan Society of Mechanical Engineers. C, **64**, 9, (1998), 3596–3602 (in Japanese)

[3] T. Ishida, S. Huang, T. Hidaka, M. Sasahara, and A. Maruyama: Rotational Transmission Errors of Strain Wave Gearing(Experimental Study), Transactions of the Japan Society of Mechanical Engineers. C, **61**, 12, (1995), 4776–4784 (in Japanese)

[4] S. Yanabe, A. Ito, A. Okamoto, T. Yamaguch, M. Ikeda, and H. Fujita: Rotational Transmission Error of Harmonic Drive Device, Transactions of the Japan Society of Mechanical Engineers. C, **56**, 1, (1990), 148–153 (in Japanese)

[5] H. Ishizaki, T. Nishino, N. Okada, N. Oshima, T. Fukuda, and T. Kanzawa: Instability Phenomena of the Rotor(2nd Report), Report of the National Astronomical Observatory of Japan, **3**, (1998), 117–113 (in Japanese)

[6] H. D. Taghirad, and P. R. Bélanger: Modeling and Parameter Identification of Harmonic Drive Systems, Journal of Dynamic Systems, Measurement and Control, **120**, 12, (1998), 439–444

[7] T. Mizuno, M. Yamamoto, M. Iwasaki, M. Kawahuku, H. Hirai, Y. Okitsu, K. Sasaki, and T. Yajima: Mathematical Modeling for Angular Transmission Error by Gear Accuracy of Harmonic Drive Gearing, Tokai-Section Joint Conference of the 8 Institutes of Electrical and related Engineers, O-140, (2007) (in Japanese)

[8] M. Yamamoto, M. Iwasaki, H. Hirai, Y. Okitsu, K. Sasaki, and T. Yajima: Modeling and Compensation for Angular Transmission Error in Harmonic Drive Gearings, *IEEJ Transactions on Electrical and Electronic Engineering*, **4**, 2, (2009), pp.158–165

[9] M. Itoh, and S. Kasei: Suppression of Transient Vibration for Geared Mechanical System : Effects of Model-Based Control, Transactions of the Japan Society of Mechanical Engineers. C, **64**, 7, (1998), 2596–2601 (in Japanese)

[10] N. Takesue, J. Furusho, and K. Fujinaga: Control Using Joint Sensor of Robot Arm with Two-Inertia Resonance –Comparison with Control Using State-Estimation Observer–, IEEJ Trans. IA, **124**, 10, (2004), 985–993 (in Japanese)

[11] T. Hidaka, T. Ishida, Y. L. Zhang, H. Sentoku, M. Sasahara, and Y. Tanioka: Theoretical Analysis of the Vibration in a Robot due to a Strain Wave Gearing, Transactions of the Japan Society of Mechanical Engineers. C, **55**, 8, (1989), 1864–1871 (in Japanese)

[12] R. Dhaouadi, F. H. Ghorbel, and P. S. Gandhi: A New Dynami Model of Hysteresis in Harmonic Drives, IEEE Transaction on Industrial Electronics, **50**, 6, (2003), 1165–1171